Theory of a two-stage hypervelocity launcher to give constant driving pressure at the model

By F. SMITH

The War Office, Royal Armament Research and Development Establishment, Fort Halstead, Kent

(Received 6 December 1962 and in revised form 11 March 1963)

The increase in hypervelocity launcher velocities, the tendency for models to become more fragile and the use of sabot techniques has made it increasingly more important to reduce peak accelerations during the launch phase. At the same time a high acceleration must be maintained to enable a launcher barrel of reasonable length to be used. This paper considers the theoretical design of a launcher to give constant acceleration to the model. A similarity solution is found for the launcher barrel and the solution is extended to the first stage of the launcher. Departure from ideal gas laws is also discussed and the theory is extended to include the effect of molecular volume. The motion of the driving piston in the first stage is considered in detail and techniques to ensure that the piston motion results in constant base pressure on the model are presented.

1. Introduction

The design and development of launchers to accelerate models up to 20,000 ft./sec started several years ago. In many laboratories in U.S.A. and Canada use has been made of chemical propellants, explosives, oxygen-hydrogen combustion or combinations of these to supply energy to the first stage of two-stage launchers. Other simpler approaches have used explosives or shaped charges accelerating the model directly, although in these cases the model is often of unknown mass and shape.

We started at R.A.R.D.E. in 1957 on the theoretical design of a launcher to achieve velocities of the same order of magnitude (Smith 1958), the chief difference in our approach being to use light gases at high pressures but room temperatures. The advantages of this approach are that relatively conventional engineering techniques are used and that gases of known composition and at known pressure lead to an easier theoretical design. The disadvantages lie in the less convenient handling of the energy source and the time needed to charge pressure vessels to a high pressure.

Launchers designed some years ago have been developed to give velocities higher than the design velocity, possibly because, as this paper will show, imperfect gas effects are favourable. At R.A.R.D.E. velocities exceeding 30,000 ft./sec have been achieved, and the author is aware of two laboratories in the U.S.A. where this figure has also been exceeded. In spite of this development there is a need for still higher velocities in order to simulate upper atmosphere

and space flight, and to advance the understanding of hypervelocity impact. At the same time, this need for higher velocities is coupled with a need for more complex models which are difficult to accelerate without damage.

These requirements led Charters & Curtis (1962) to propose a launcher based on an extruding piston and designed to give a constant base pressure at the model. Some preliminary results by the method of characteristics have been obtained on a high-speed computer. The object of the present paper is to present a similarity solution to the problem of constant base pressure. The solution is extended to the complete design of a two-stage light gas launcher.

2. Similarity solution for a perfect gas

The general arrangement of the two-stage launcher is shown in figure 1, where the descriptive suffices o, r, s, i are defined.

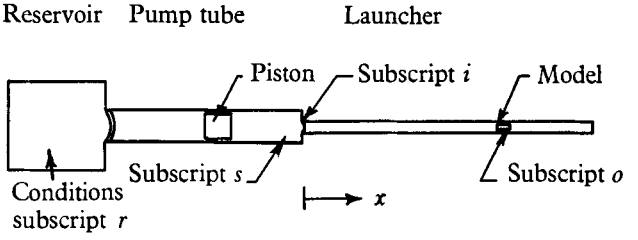

FIGURE 1. General design of light gas launcher.

Let us consider the usual equations of unsteady flow in a duct of constant area. In the launcher barrel, we have

$$\frac{\partial \rho}{\partial t} + u\frac{\partial \rho}{\partial x} + \rho\frac{\partial u}{\partial x} = 0, \tag{1}$$

$$\frac{\partial u}{\partial t} + u\frac{\partial u}{\partial x} = -\frac{1}{\rho}\frac{\partial p}{\partial x}, \tag{2}$$

where ρ is density, u velocity and p pressure.

These equations can be re-written as the well-known characteristic equations (see equation (6) below)

$$\frac{\partial}{\partial t}\left[\frac{2a}{\gamma-1} \pm u\right] + (u \pm a)\frac{\partial}{\partial x}\left[\frac{2a}{\gamma-1} \pm u\right] = 0, \tag{3}$$

where $a = (\gamma p/\rho)^{\frac{1}{2}}$ is the speed of sound.

Let us look for a similarity solution of the form

$$u = U(t). \tag{4}$$

If such a solution applies then all gas particles will have the same velocity as the model at any given time. Substituting (4) into (1) and (2) we find that

$$u = \alpha t \tag{5}$$

is such a solution. With the use of

$$p/\rho^{\gamma} = \text{const.} \tag{6}$$

we find that

$$a^2 = \text{const.} + \tfrac{1}{2}(\gamma-1)\,\alpha^2 t^2 - (\gamma-1)\,\alpha x. \tag{7}$$

This similarity solution has been given by Stanyukovitch (1960). At the model we have

$$x = \frac{1}{2}\frac{p_0 A_0}{m_0} t^2, \tag{8}$$

assuming p_0 constant. Here A denotes cross-sectional area. If we choose $\alpha = p_0 A_0/m_0$ then, at the model, $a_0^2 = \text{const.}$ This is consistent with constant p_0, so that the similarity solution

$$u = \frac{p_0 A_0}{m_0} t \tag{9}$$

is consistent with constant pressure on the model. If the conditions a_0, p_0, m_0, A_0 at the model are taken as reference and the definitions

$$\bar{x} = x\frac{p_0 A_0}{a_0^2 m_0}, \quad \bar{t} = t\frac{p_0 A_0}{a_0 m_0}, \quad \bar{u} = \frac{u}{a_0} = \bar{t}, \tag{10}$$

are introduced, equation (7) can then be expressed non-dimensionally as

$$\bar{a}^2 = 1 + \tfrac{1}{2}(\gamma-1)\,\bar{t}^2 - (\gamma-1)\,\bar{x}. \tag{11}$$

We also have

$$\bar{p} = \bar{a}^{2\gamma/(\gamma-1)}, \quad \bar{\rho} = \bar{a}^{2/(\gamma-1)}. \tag{12}$$

2.1. *Conditions at launcher entry*

Using suffix i to denote conditions just downstream of the inlet to the launcher barrel where $x = 0$, we have

$$\bar{u}_i = \bar{t}_i, \tag{13}$$

$$\bar{a}_i^2 = 1 + \tfrac{1}{2}(\gamma-1)\,\bar{t}_i^2, \tag{14}$$

$$\bar{p}_i = [1 + \tfrac{1}{2}(\gamma-1)\,\bar{t}_i^2]^{\gamma/(\gamma-1)}, \tag{15}$$

$$\bar{\rho}_i = [1 + \tfrac{1}{2}(\gamma-1)\,\bar{t}_i^2]^{1/(\gamma-1)}. \tag{16}$$

The mass $\bar{m}_l$ of gas in the launcher barrel is given by

$$\frac{m_l}{m_0} = \bar{m}_l = \bar{p}_i - 1 = [1 + \tfrac{1}{2}(\gamma-1)\,\bar{t}_i^2]^{\gamma/(\gamma-1)} - 1. \tag{17}$$

In the two-stage light-gas launcher the supply of gas to the barrel at the correct rate, i.e. at the correct mass flow and pressure, is provided by the pump-tube piston acting on the driving gas (figure 1). It is now assumed that the flow in the pump tube is steady and one-dimensional with no aerodynamic loss at the entry to the launcher barrel. At the entry the energy equation for steady subsonic flow is

$$\frac{2}{\gamma-1}\bar{a}_i^2 + \bar{u}_i^2 = \frac{2}{\gamma-1}\bar{a}_s^2 + \bar{u}_s^2. \tag{18}$$

Provided the area ratio $\bar{A}_s$ ($= A_s/A_0$) is sufficiently large $\bar{u}_s$ can be neglected.

Then from equation (14),

$$\bar{a}_s^2 = 1 + (\gamma-1)\,\bar{t}_i^2 = \bar{p}_s^{(\gamma-1)/\gamma} = \bar{\rho}_s^{(\gamma-1)}. \tag{19}$$

After sonic conditions have been reached, the velocity at the launcher entry is limited to the local sonic value, and it is no longer possible to match the entry requirements of the similar solution. It will be assumed that the similar solution for the greater part of the launcher barrel is linked to the sonic condition at the entry by an unsteady flow up to the limiting characteristic, Q, which corresponds to the first time at which sonic flow was reached at the throat.

Then equation (19) is replaced for sonic entry flow by

$$\bar{a}_s^2 = \tfrac{1}{2}(\gamma+1)\,\bar{a}_i^2, \tag{20}$$

where $\bar{a}_i$ is given by the characteristic solution.

The characteristics of the similar solution are given by

$$P, Q = \frac{2}{\gamma-1}\bar{a} \pm \bar{u} = \text{const.}, \tag{21}$$

and their respective velocities are $\bar{u} \pm \bar{a}$. From equations (21) and (11) a unique characteristic diagram can be obtained (as in figure 2 for $\gamma = 1{\cdot}4$).

From these unique solutions, which are similar to the sonic point and similar-characteristic beyond this point, a non-dimensional chart relating $\bar{a}_0$, $\bar{u}_i$, $\bar{t}_i$, $\bar{m}_l$, $\bar{p}_i$ and $\bar{p}_s$ can be constructed. Figure 3 shows such a chart for $\gamma = 1{\cdot}4$. The sonic point is marked to indicate the transition from one solution to the other and an example is shown (by arrows) to illustrate the relation between the curves. The variation of $\bar{m}_l$ and $\bar{p}_s$ with time can be used to analyse the motion of the pump-tube piston.

For convenience the gas-dynamic parameters in the pump tube will be expressed in terms of V_s, the volume in front of the piston, and $m_g - m_l$, the mass of gas in the pump tube at any given time. Thus we have

$$\rho_s V_s = m_g - m_l, \tag{22}$$

or, with

$$\bar{V}_s = \frac{V_s p_0}{a_0^2 m_0},$$

we have

$$\gamma \bar{a}_s^{2/(\gamma-1)} \bar{V}_s = \bar{m}_g - \bar{m}_l. \tag{23}$$

From the foregoing equations and figure 3, $\bar{a}_s$, $\bar{m}_g$, $\bar{m}_l$ can be obtained, giving the variation of $\bar{V}_s$ with time.

This is the matching condition for the flow required by the launcher barrel. We will now assume that the volume change is produced by the pump-tube piston of mass m_p ($= \bar{m}_p m_0$). Obviously, the motion of this piston will be governed primarily by the back pressure p_s in the pump tube, particularly in the final stages of the motion where the driving pressure p_p is very much smaller than p_s. Taking A_s as constant we have

$$\frac{\bar{p}_s \bar{A}_s^2}{\bar{m}_p} = \frac{d^2 \bar{V}_s}{d\bar{t}^2},$$

or

$$\bar{V}_s = \frac{\bar{A}_s^2}{\bar{m}_p} \iint \bar{p}_s \, d\bar{t} \, d\bar{t} + K_1 \bar{t} + K_2. \tag{24}$$

Equation (24) must give the same value for $\bar{V}_s$ as equation (23) in order that the pump-tube piston shall drive the model with a constant base pressure at the

model. In order to match equations (23) and (24) we have three parameters available, i.e. K_1, K_2, $\bar{A}_s^2/\bar{m}_p$.

The technique of matching will be discussed in a later section.

However, the theory so far has been for an ideal gas with $\gamma = 1{\cdot}4$; we must now consider the effect of gas imperfections.

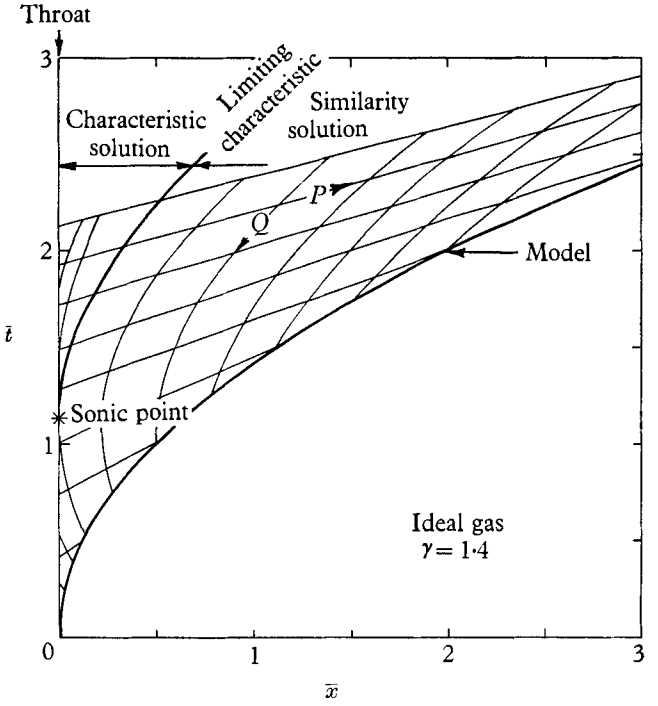

FIGURE 2. Characteristics behind model.

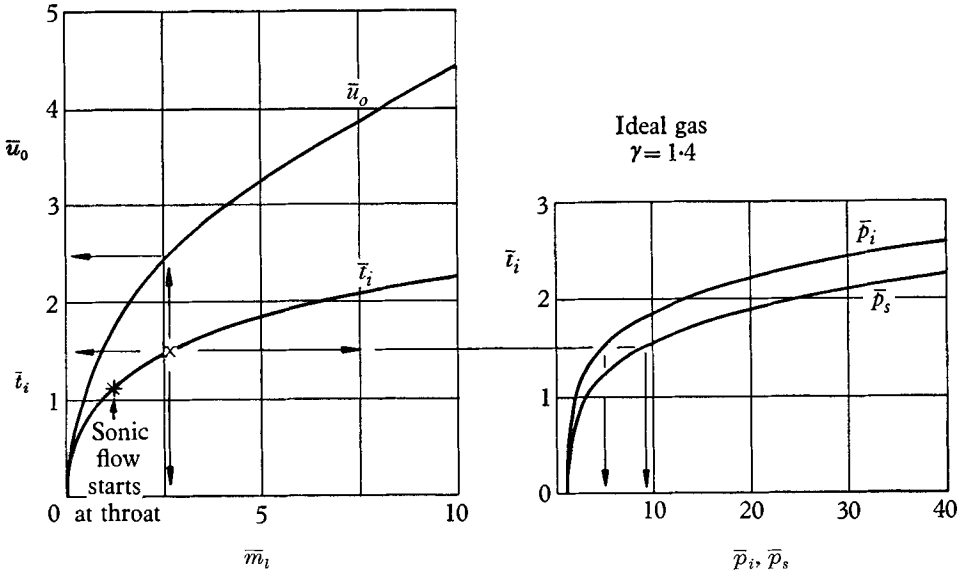

FIGURE 3. Non-dimensional chart for $\bar{m}_l$, $\bar{t}_i$, $\bar{u}_0$, $\bar{p}_i$, $\bar{p}_s$.

3. Similarity solution for an imperfect gas

In view of the high temperature and very high pressures in the pump tube and launcher barrel, we must consider deviations from the ideal gas laws used in §2. Dissociation and ionization effects will be ignored for hydrogen since under the conditions practically obtainable in a light gas launcher these effects are negligible. The imperfect gas relations are given in a report by the staff of the Ames Laboratory, N.A.C.A. (1953). The principal imperfections to be considered are due to molecular volume, molecular attraction and molecular vibration. Molecular attraction is easily shown to be unimportant when the pressure is much greater than the critical pressure. Corrections for molecular vibration lead to very intractable equations and are best dealt with by a step-by-step method. Typical calculations have shown that the corrections due to molecular vibration do not significantly affect the motion of the model and the pump-tube piston for $T_{\max} < 4000\,^{\circ}\mathrm{K}$, although possible effects should be checked for any particular launcher design. Therefore only the effect of molecular volume will be considered here.

The gas equations with the effect of molecular volume included are

$$p(v-b) = RT, \quad p(v-b)^{\gamma} = \text{const.}, \quad a^2 = \frac{\gamma p v^2}{v-b}, \tag{25}$$

where γ has the perfect gas value, v is the specific volume and b is the molecular volume.

Equations (2) and (3) are now replaced by

$$\frac{\partial u}{\partial t} + u\frac{\partial u}{\partial x} + \frac{2}{\gamma-1} w \frac{\partial w}{\partial x} = 0, \tag{26}$$

$$\frac{\partial}{\partial t}\left(\frac{2c}{\gamma-1} \pm u\right) + (u \pm a)\frac{\partial}{\partial x}\left(\frac{2c}{\gamma-1} \pm u\right) = 0, \tag{27}$$

where $w^2 = p(\gamma v - b)$, $c^2 = \gamma p(v-b)$. (For an ideal gas, $a = c = w = \gamma p v$.) At the throat the energy equation is now

$$u^2 + \frac{2}{\gamma-1} w^2 = \text{const.} \tag{28}$$

We may arbitrarily choose either a_0, c_0 or w_0 to produce non-dimensional coefficients. Since the energy equation links the steady to unsteady flow at the throat it is appropriate to choose w_0. Terms involving w_0 in their non-dimensional form will be denoted by a tilde, e.g. $\tilde{a} = a/w_0$. Thus we get

$$\tilde{a}^2 = \frac{\bar{p}^{(\gamma-1)/\gamma}}{1-Y}\left[1 + Y\left\{\frac{\gamma}{\gamma-1}\bar{p}^{1/\gamma} - 1\right\}\right]^2, \tag{29}$$

$$\tilde{c}^2 = \bar{p}^{(\gamma-1)/\gamma}(1-Y), \tag{30}$$

$$\tilde{w}^2 = \bar{p}^{(\gamma-1)/\gamma}[1 - Y + Y\bar{p}^{1/\gamma}], \tag{31}$$

where

$$Y = \frac{(\gamma-1)bp_0}{w_0^2}. \tag{32}$$

The energy equation becomes

$$\tilde{w}^2 = 1 + \tfrac{1}{2}(\gamma-1)\tilde{t}^2 - (\gamma-1)\tilde{x}. \tag{33}$$

At the throat $$\tfrac{1}{2}(\gamma-1)\tilde{t}_i^2 = (1-Y)[\bar{p}_i^{(\gamma-1)/\gamma} - 1] + Y(\bar{p}_i - 1), \tag{34}$$

and using the characteristic equations

$$\tilde{u}_0 - \tilde{u}_i = \frac{2}{\gamma-1}(\tilde{c}_i - \tilde{c}_0) = \left(\frac{2}{\gamma-1}\right)(1-Y)^{\frac{1}{2}}[\bar{p}_i^{(\gamma-1)/2\gamma} - 1]. \tag{35}$$

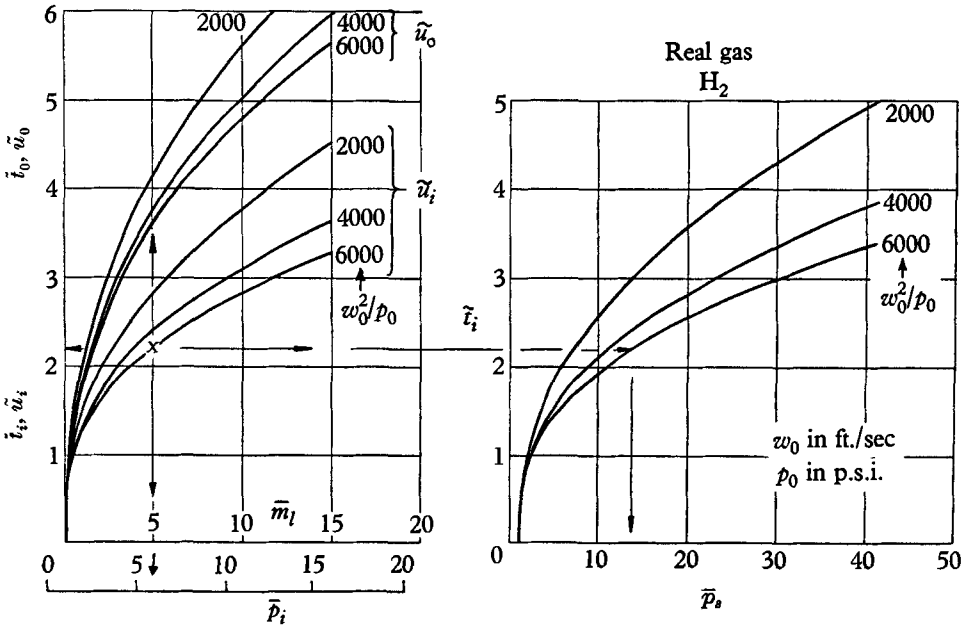

FIGURE 4. Non-dimensional chart for $\bar{m}_l, \tilde{t}_i, \tilde{u}_0, \bar{p}_i, \bar{p}_s$.

It can be seen from equations (25) that the effect of molecular volume is to increase the value of the speed of sound above its perfect gas value and thus increase the value of $\tilde{t}_i$ at which sonic flow is reached at the throat. If the initial value of the specific volume, v_0, is sufficiently small the flow remains subsonic at the throat. For hydrogen this corresponds to $w_0^2/p_0 < 6500$ for $\bar{p} < 20$, where w_0 is measured in ft./sec and p_0 in lb./in.^{2}. Outside this limit a characteristic solution must be calculated near the throat.

With the energy equation (28) and ignoring u_s as before we have

$$\tilde{w}_s^2 = 2\tilde{w}_i^2 - 1, \tag{36}$$

and $$(1-Y)(\bar{p}_s^{(\gamma-1)/\gamma} - 1) + Y(\bar{p}_s - 1) = 2(1-Y)(\bar{p}_i^{(\gamma-1)/\gamma} - 1) + 2Y(\bar{p}_i - 1). \tag{37}$$

Using equations (29) to (37) we can now construct non-dimensional charts for a real gas with the effect of the molecular volume included. Figure 4 shows such a chart for hydrogen with $\gamma_{\text{perfect}} = 1{\cdot}415$. Y (or w_0^2/p_0) is an added variable and a practical range of w_0^2/p_0 of 2000–6000 has been taken; w_0 is expressed in ft./sec, p_0 in lb./in.^{2}.

Comparison with figure 3 shows that substantial increases in velocity and reductions in peak pressure result from including the molecular volume. Physically, this is because it is difficult to force gas of a limited minimum volume into the launcher barrel, and as a result the pressure at the throat, which is non-dimensionally equal to the mass of gas and model combined, is substantially

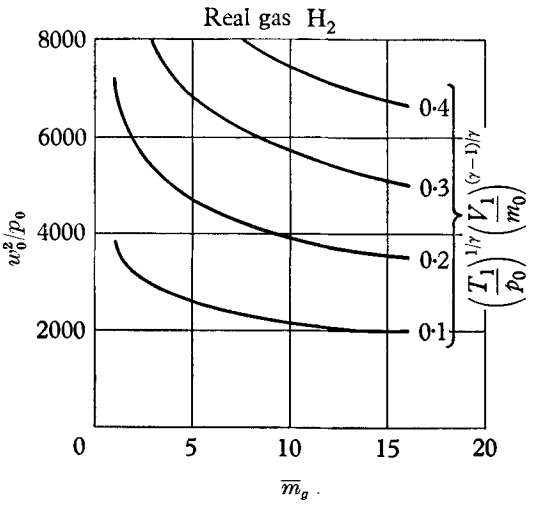

FIGURE 5. Pump-tube charging conditions (T_1 = initial temperature in pump tube; V_1 = initial volume of pump tube).

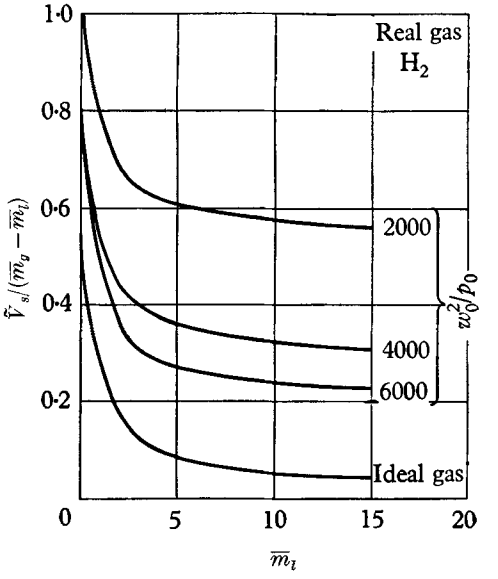

FIGURE 6. Chart relating $\tilde{V}_s$ and $\overline{m}_l$.

reduced. This is somewhat offset by the increase in the speed of sound, which reduces the time required to transmit pressure changes from the throat to the model. Consequently the drive at the throat must be maintained for a longer time for the last characteristic to reach the model as it leaves the launcher. Further, the relation between pressures in the stagnation region and the throat leads to a much reduced peak pressure.

Two further charts are given in figures 5 and 6. Figure 5 enables the initial conditions in the pump tube to be linked to the variables w_0^2/p_0 and $\overline{m}_g$ of figure 4. Figure 6 gives $\tilde{V}_s$ to assist in calculating the motion of the piston during its driving motion: here

$$\tilde{V}_s = (\overline{m}_g - \overline{m}_l) f\left(\frac{w_0^2}{p_0}, \overline{m}_l\right), \tag{38}$$

and

$$\tilde{V}_s = \frac{\bar{A}_s^2}{\overline{m}_p} \int\int \bar{p}_s d\tilde{t} d\tilde{t} + K_1 \tilde{t} + K_2. \tag{39}$$

4. Matching of piston motion

As discussed in §§ 2 and 3 the piston motion has to satisfy the mass-flow requirement of the barrel as indicated by full lines in figures 7 and 8. The design parameters are the mass m_p of the pump-tube piston, the pump-tube area A_s and

the velocity of the piston when the model starts to move. These parameters appear as $\bar{m}_p/\bar{A}_s^2$, K_1, K_2 in equation (39). The broken curves in figures 7 and 8 show the result of attempting to match the requirements for ideal and real gases respectively. It will be seen that the match is reasonably good and the curves give the mass $\bar{m}_g$ of gas required, the mass $\bar{m}_p$ of the piston, and the piston velocity from the initial slope of the pressure curve. Where the curves do not match

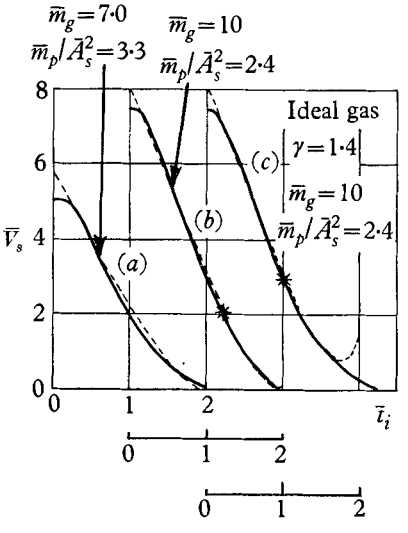

FIGURE 7

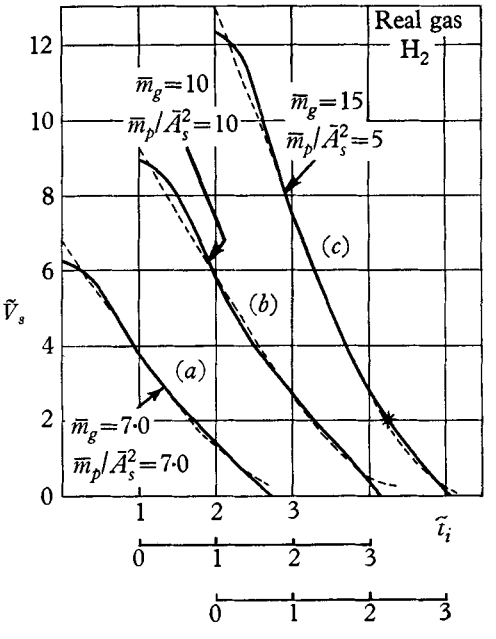

FIGURE 8

FIGURE 7. Matching of mass flow and pressure requirements for piston motion. (*a*) Simple match; (*b*) excess gas compared with (*a*) with 100% gas leakage starting at $\bar{t}_i = 1{\cdot}2$; (*c*) excess gas and straight taper extrusion to throat starting at $\bar{V}_s = 3$. ——, Mass flow requirement; ···, pressure requirement.

FIGURE 8. Matching of mass flow and pressure requirements for piston motion. (*a*) Simple match; (*b*) simple match; (*c*) excess gas compared to (*b*) and port of unit volume at $\tilde{V}_s = 2$. ——, Mass flow requirement; ···, pressure requirement. $w_0^2/p_0 = 4000$.

neither is correct, the true piston motion being a compromise between the two curves. However, for a real gas, towards the end of the piston motion, the gas behaves more like a liquid than a gas so that the piston motion will be nearer to the mass flow requirement curve than to the pressure requirement curve.

Since a mismatch between these requirements will result in a change of pressure at the base of the model, it is desirable to attempt a better matching of the two curves. To do this we require more variables than the three so far available and this can be achieved either by adjustment of the mass of gas during the piston motion, or by an adjustment of the effective piston mass, or by a combination of both.

Dealing first with gas control we can start with an excess of gas and either allow a controlled leakage—by bursting diaphragms for example—or allow

removal of the gas from the compression—by, say, a port which is covered by the piston moving down the barrel. The first of these two methods leads to a reduction of piston deceleration and its effect is shown in figure 7, curve (*b*), for an ideal gas. Here a simple gas leakage with a cross-sectional area equal to the launcher barrel area (100 % leakage) starts at $\bar{V}_s = 2$, and it can be seen that this results in a very good match for the piston requirements. A more complicated gas-leakage system could result in an even better match and, further, it is often possible to arrange that the piston will reach the end of barrel with zero velocity. This, of course, implies a slight loss in performance since the correct conditions cannot then be maintained right up to the throat.

This solution is excellent for an ideal gas, or real gas up to moderate peak pressure. However, for a real gas at high peak pressures the mass-flow requirement becomes linear with time (or even increasing with time at extremely high pressures), resulting in the need for a constant piston velocity at the end of the stroke. In this case gas control is better applied by the 'port' method where the excess gas is trapped at a pre-arranged part of the piston stroke. Figure 8, curve (*c*), shows how the mass flow curve can be given an artificial curvature by, in this example, trapping one-third of the gas at $\bar{V}_s = 2$. Further ports could improve the match of the two curves and result in zero piston velocity at the end of the stroke. In some ways this method of gas control is the simpler one because it is predetermined. It is, in any case, often necessary to have mechanical seals in the pump tube and it is difficult to make these seals perfect at the high rates of strain in the pump tube. Thus it may often be possible to make a virtue out of a necessity.

The other method of control of piston motion is by control of the deceleration. This method has been applied by Charters & Curtis (1962) by tapering the end of the pump tube so that the piston is squeezed down to the diameter of the launcher barrel. Treating the piston (of plastic) as an incompressible fluid, we have in the piston

$$\frac{\partial p}{\partial x} = -\rho_p \frac{du}{dt},$$

which gives

$$\frac{p_p}{\rho_p} + \tfrac{1}{2}u_p^2 - \left(\frac{p_s}{\rho_p} + \tfrac{1}{2}u_s^2\right) = \frac{du_p}{dt}[l_p + l_t(X^{\frac{1}{2}} + \tfrac{1}{3}X^{-\frac{3}{2}} - \tfrac{4}{3})], \tag{40}$$

where ρ_p is the piston density, p_p and p_s are the piston pressures on the rear and front faces, l_p is the initial length of the piston (or equivalent length at density ρ_p), l_t is the length of taper (see figure 9), and $X = A_p/A_s$. Also

$$u_p A_p = u_s A_s. \tag{41}$$

From equation (41) it is seen that the volume change of the piston is the same front and rear so that tapering of the pump tube does not alter the volume sweep of the piston, which has been seen in equations (23), (24), (38) and (39) to be the important variable in the piston motion. However, accepting this, we see from equation (40) that the effective back pressure of the piston is affected by two factors: first, the increase in $\frac{1}{2}\rho_p u^2$ from rear to front of the piston and, second, the change in the apparent mass of the piston (the right-hand side of (40)). Of

these two effects the first is by far the most powerful. For example, if a polythene piston is extruded at 2000 ft./sec without loss of velocity from 1 to $\frac{1}{4}$ in. diameter the increased back pressure is 8×10^6 lb./in.^{2}. Thus, taper is a powerful means of slowing down a piston.

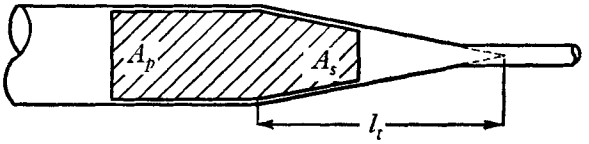

FIGURE 9. Tapered pump tube with extruding piston.

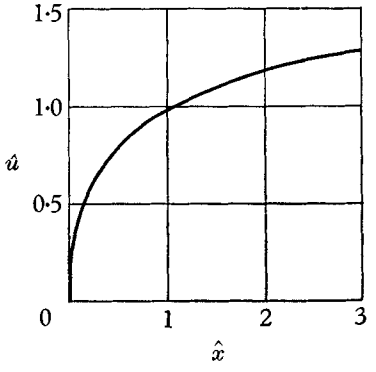

FIGURE 10. Piston acceleration, helium driving

The result of a typical ideal gas calculation is shown in figure 7, curve (c), where a tapered piston results in a good match up to $\bar{l}_t = 1{\cdot}6$. Beyond this point, however, the taper effect is far too powerful and so the taper should be ended at this point. However, if the taper were ended we should lose one of the main advantages of the extruding piston, namely that it avoids unacceptable damage if a piston strikes the end of the pump tube.

To sum up, gas leakage, gas trap, or moderate taper are all satisfactory ways of dealing with mismatch. Gas leakage and taper apply for an ideal gas or a real gas at moderate pressures. Only the gas trap effect applies to a real gas at high pressures. In some cases gas control may enable the piston to be brought to rest at the end of the barrel, but in other cases taper to the launcher barrel may be the only practical way of avoiding damage, although with some loss of performance.

5. Piston acceleration—initial motion

The acceleration of the piston can be most simply treated by ignoring the pressure in front of the piston. The errors due to this assumption are small and can in any particular case be removed by a more detailed calculation. What is required here is an over-all view of the piston motion. The equation of motion is

$$\hat{x} = \frac{\hat{u} - [2/(\gamma+1)]\,K_3}{(K_3 - \frac{1}{2}(\gamma-1)\,\hat{u})^{(\gamma+1)/(\gamma-1)}} + \frac{2}{\gamma+1}\,\frac{1}{K_3^{2/(\gamma-1)}}, \tag{42}$$

where $\hat{x} = p_r A_p x/m_p a_r^2$, $\hat{u} = u/a_r$, and K_3 is a factor associated with the reflexion of characteristics from the reservoir throat (Smith 1958). For helium as the driver gas ($\gamma = \frac{5}{3}$), we have $K_3 = 1{\cdot}1$, so that

$$\hat{x} = \frac{\hat{u} - 0{\cdot}825}{(1{\cdot}1 - \frac{1}{3}\hat{u})^4} + 0{\cdot}562. \tag{43}$$

This relation is shown in figure 10, and it will be seen that for practical purposes the piston velocity is limited to a maximum near the sonic speed for helium. In turn this will determine the area ratio $\bar{A}_s$ in the $(\bar{V}_s, \bar{t}_i)$ relations (figure 8).

6. Limitations of the theory

Apart from the theoretical limitations mentioned throughout the paper there are a number of known practical limitations which are difficult, if not impossible, to include in any theory. These limitations can be summarized as follows:

(i) *Boundary layer.* It has been assumed that boundary-layer effects are negligible. If, in fact, these effects are considerable the distribution of velocity across the launcher barrel will no longer be constant and the similarity solution will no longer be valid.

(ii) *Friction.* No allowance has been made for friction either on the model or the piston. Little is known about friction of plastics such as nylon and polythene at high velocities. No effects have been noted to date.

(iii) *Plastic deformation of barrels.* Peak pressures on the pump tube and the launcher barrel are well beyond the elastic limits of any material. In principle the high-pressure tube can be designed to hold the pressure but the plastic flow on the inside of the barrels may prove a limitation.

(iv) *Gas erosion.* This has already been a serious problem with helium as the driver gas for the model. A substantial improvement has resulted from the use of hydrogen, due to the reduction of temperature and heat transfer but as higher velocities are obtained the problem must again become a serious one.

(v) *Contamination of gas.* Contamination of the hydrogen results in a loss of performance. Erosion may result in gas contamination.

(vi) *Damage due to piston striking the end of the pump tube.* This problem has been mentioned in § 4. It may not always be possible to avoid high pressures from this cause, and some method of damage avoidance may be necessary.

(vii) *Size and cost.* Launchers for high velocity and a reasonable size of model are bound to be large and costly. It may be that higher velocities can only be achieved without prohibitive expense by a reduction in model size.

7. Conclusions

A similarity solution for the design of a two-stage hypervelocity launcher has been presented. It should be possible to design a launcher for a particular velocity and model size from theory. There is no theoretical limit of performance; larger launchers will give higher velocities and the achievable velocity will be set by practical rather than theoretical limitations.

Methods of designing for correct piston performance have been discussed and the limitations of piston extrusion have been described.

The author wishes to thank Mr D. F. T. Winter for many useful discussions.

REFERENCES

AMES LABORATORY RESEARCH STAFF 1953 Equations, tables and charts for compressible flow. *NACA Rep.* no. 1135.

CHARTERS, A. C. & CURTIS, J. S. 1962 High velocity guns for free flight ranges. *Defence Research Laboratories, General Motors Corporation,* TM 62-207.

SMITH, F. 1958 Unpublished Ministry of Supply Report.

STANYUKOVITCH, K. P. 1960 *Unsteady Motion of Continuous Media* (ed. M. Holt), pp. 605–607. London: Pergamon Press.